

**(2E)-3-(1-benzothiophen-2-yl)-1-(4-hydroxyphenyl)prop-2-en-1-one:
Synthesis, Characterization (IR, NMR and UV-Vis)
DFT Study and Antimicrobial Activity**

¹Nevin Süleymanoğlu*, ²Reşat Ustabaş, ³Fatih Eydurhan, ⁴Şahin Direkel, ⁵Yasemin Ünver, ⁵Nuran Kahrıman

¹Vocational School of Technical Sciences, Gazi University, 06374 Ostım, Ankara, Turkey.

²Department of Mathematics and Science Education, Educational Faculty, Ondokuz Mayıs University, 55139 Kurupelit, Samsun, Turkey.

³Department of Chemistry, Faculty of Arts & Sciences, Adnan Menderes University, 09100, Aydın, Turkey.

⁴Department of Medical Microbiology, Faculty of Medicine, Giresun University, 28100 Giresun, Turkey.

⁵Department of Chemistry, Faculty of Sciences, Karadeniz Technical University, 61080 Trabzon, Turkey.

nevinseylan@gmail.com*

(Received on 19th January 2021, accepted in revised form 1st June 2021)

Summary: In this study new chalcone derivative (2E)-3-(1-benzothiophen-2-yl)-1-(4-hydroxyphenyl)prop-2-en-1-one (I), which has important pharmacological applications, was designed and synthesized. IR, NMR and LC-MS/MS empirical methods were used in order to confirm the molecular structure of the synthesized compound I. Both two tautomeric forms of the molecule were optimized by using density functional theory (DFT) method. The structural parameters formed after optimization and structural parameters obtained from similar compounds by X-ray diffraction show a good correlation. The theoretical and experimental results of IR and NMR are generally compatible, but difference arises between some values. This difference shows the existence of O–H...O type intermolecular hydrogen bond. By using its UV-Vis data, the visible absorption maximums of the molecule were analyzed. Compound I was tested against kind of *Leishmania major* from the point of antileishmanial activity, against kind of *Candida albicans* from the point of antifungal activity and against fourteen kinds of bacteria from the point of antibacterial activity in this study. The test results showed, that compound I was effective on eight kinds of bacteria and the activity strength on six bacteria among the eight was MIC: 5000 µg/mL and on the rest two kinds MIC: 1250 µg/mL. Besides, it was also found out, that compound I has MIC: 5000 µg/mL antileishmanial activity. Since bacterial and parasitic infections form serious health problems globally, compound I may be a medication candidate in future; if its antibacterial and antiparasitic effect are taken into consideration.

Keywords: Chalcone, FTIR-NMR, UV-Vis, DFT study, Antimicrobial activity, *Leishmania major*.

Introduction

Chalcones (1,2-diaryl-2-propene-1 ones) and their derivatives are drawing attention due to many important pharmacological applications and properties [1]. Chalcones are the main pioneers of biosynthesis isoflavonoids and flavonoids and they are present in nature from ferns to higher plants [1, 2]. Both natural and synthetic chalcones exhibit diverse biological activities such as antimalarial, anti-tuberculosis agents, antioxidant, antileishmanial agents, antiviral, antiplatelet, anti-inflammatory, Tubulin inhibitors, antibacterial, DNA gyrase inhibitor, antiulcer, antimycotic, reverse-transcriptase inhibitor, cardiovascular, antifungal and antitumor [1-3]. Chalcones are well-known intermediates thanks to their reactive α,β -unsaturated carbonyl moiety and it makes important for the synthesis of various heterocyclic and bioactive compounds like pyrimidines, pyrazolines, quinolinones, ispxazoles, benzofuranones, flavones and epoxides [4-6].

Bacterial infections create a big threat for the global health [7]. Exploration of antibiotics, that are

used to treat bacterial infections, is one of the biggest success in medical field [8]. However, due to the misuse of antibiotics, bacteria developed resistance to antibiotics. Thus, necessity of new antibiotics increase dynamically [9].

Leishmaniasis is a disease which infects humans through a bite of sand fly and has its source in intracellular parasite [10]. It is a disease, which affects humans and various mammals. Geographical distribution of this disease comprise about 90 countries around the world [11]. Every year, about 1,5-2 million new incidence comes out 500000 of these incidences are in visceral and 1500000 are in (muko) cutaneous form [12]. Up to the present no vaccine was licensed, that can be used on humans against any form of leishmaniasis [13]. This situation brings globally an important health problem into existence.

The goal of this study was to synthesize the new chalcone derivative (2E)-3-(1-benzothiophen-2-yl)-1-(4-hydroxyphenyl)prop-2-en-1-one (I) and

*To whom all correspondence should be addressed.

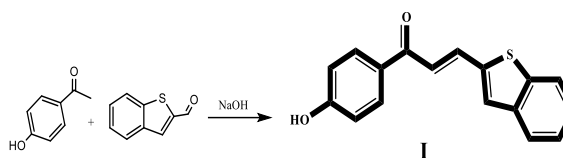
search its antibacterial, antifungal and antiparasitic activities, since chalcones and their derivatives have important pharmacological applications. For this purpose, IR, NMR and LC-MS/MS empirical methods were used in order to confirm the molecular structure of the synthesized compound. To obtain the molecular geometry and spectroscopic parameters of compound I, theoretical approach at B3LYP/6-311G++(d,p) level were used and the structural characteristics of compound I were compared with geometric parameters of compounds with similar structure. Antimicrobial activities were evaluated in vitro by measuring minimum inhibitory concentration (MIC). These days, since the bacterial infections and parasites create important health problems globally, this study may be a contribution in improving antibacterial and antiparasitic medicaments.

Experimental and Computational Method

Synthesis of (2E)-3-(1-benzothiophen-2-yl)-1-(4-hydroxyphenyl)prop-2-en-1-one (I)

Different methods are available for the synthesis of chalcones in the literature [1]. The most known and traditional obtainment method is Claisen-Schmidt condensation carried out in basic or acidic media under homogeneous conditions. In this study, (2E)-3-(1-benzothiophen-2-yl)-1-(4-hydroxyphenyl)prop-2-en-1-one (chalcone) was produced by the reaction between 4'-hydroxyacetophenone and 1-benzothiophen-2-carbaldehyde in basic condition according to Claisen-Schmidt condensation [1-3].

To a stirred solution of 4'-hydroxyacetophenone (5 mmol) in ethanol (30 mL), 5 mL alcoholic NaOH (10 mmol) solution was added dropwise at room temperature. After mixing the reaction for 30 minutes, benzothiophen-2-carbaldehyde (5 mmol) was added to the medium in portions and the reaction mixture was stirred for 18 h. Completion of reaction was monitored by TLC and after completion it was poured in to water and acidified with HCl solution (1 N) until to pH=6.0-6.5. The obtained precipitate was filtered, washed with water and dried in the lyophilizer. The purity of yellow solid product was checked by TLC and its structure was supported spectroscopic methods (Scheme 1). Yield: 78%. M.p.: 217-219 °C. Poz. LC-MS/MS m/z (%) (C₁₇H₁₂O₂S: 280.34): 281 (74) [M+1]⁺, 263 (100) [M-OH]⁺.



Scheme-1: Synthetic pathway for the preparation of compound I.

Instrumentation

The proton and carbon Nuclear Magnetic Resonance spectra were recorded on a Bruker 400 MHz spectrometer, where TMS as an internal standard and DMSO-*d*₆ as solvent were used. IR spectrum was recorded on a Perkin-Elmer Spectrum One FTIR spectrometer. The mass spectral analysis was carried out by a Micromass Quattro LC-MS/MS spectrometer. Melting point was measured by an electrothermal apparatus.

Computational details

All quantum chemical calculations of keto and enol tautomeric forms of compound I in title were made by using Gaussian 09 [14] software package. For visualization of the calculation results, GaussView 5.0 [15] was used. The geometrical optimization of the molecule in both two tautomeric forms was realized by using DFT/B3LYP [16, 17] method and 6-311G++(d,p) basis function. Usually, there is difference between DFT oscillation frequencies and empirical oscillation frequencies. In order to compensate this difference, two different scale factors were used. For frequencies above 1700 cm⁻¹ and frequencies below 1700 cm⁻¹, 0.958 and 0.983 scaling factors were used, respectively [18, 19]. The NMR chemical shifts of the molecule in both two tautomeric forms were calculated by using GIAO [20, 21] method at DFT/B3LYP/6-311++G(d,p) level. Firstly, the optimized structures of keto and enol forms of compound I were obtained in DMSO solvent by using IEFPCM method at B3LYP/6-311++G(d, p) level and then chemical shift values were calculated in DMSO solvent. The chemical shifts of ¹H-NMR and ¹³C-NMR were scaled for B3LYP/6-311++G(d, p) level on the TMS scale by using the scale factors 31.9681 and 184.0184 ppm, respectively [22, 23]. UV absorption spectra were obtained using Time-dependent density functional theory (TD-DFT) method, by considering the optimized structures in the solvents studied [24, 25].

In vitro Antimicrobial Activities

In *in vitro* antimicrobial activity study, compound I was tested against to 14 standard bacteria, 1 fungi and 1 Leishmania isolates obtained from the American Type Culture Collection (ATCC); *Acinetobacter baumannii* ATCC 19606, *Salmonella typhimurium* ATCC 14028, *Staphylococcus aureus* (MRSA) ATCC 43300, *Klebsiella pneumoniae* ATCC 700603, *Enterobacter cloacae* ATCC 13047, *Yersinia enterocolitica* ATCC 9610, *Streptococcus agalactiae* ATCC 13813, *Citrobacter freundii* ATCC 8090, *Escherichia coli* ATCC 25922, *Enterococcus faecalis* ATCC 29212, *Haemophilus influenzae* ATCC 40247, *Listeria monocytogenes* ATCC 7644, *Streptococcus pneumoniae* ATCC 49619, *Shigella flexneri* ATCC 12022, *Candida albicans* ATCC 14053 and *Leishmania major*.

Antibacterial and Antifungal Activity

Standard bacterial/fungal isolates were incubated at 37°C throughout the night to serve them the condition for reproduction. One night awaited standard bacterial/fungal isolates were prepared according to Mc Farland 0.5/1 turbidity standards. The stock solution of the synthesized compound in solid state was first dissolved by DMSO, then water distilled up to 20000 µg/L was added to the solution and finally the solution was sterilized by filtration. As described in literature [26, 27], the dilution of compound I was realized between 5000 µg/mL and 156 µg/mL. Microplates with Alamarblue added were evaluated after 24 and 48 hours visually. Turning of Alamarblue color in wells into pink was interpreted as the growth of bacteria being in progress, whereas no change in color refer to no reproduction of bacteria. Amikacin was used as control drug for the antimicrobial test of compound I and this activity test was performed twice.

Antileishmanial Activity

The antileishmanial activity against *Leishmania major* promastigotes was defined by adding Alamarblue into the wells; in other words, by liquid microdilution method. In RPMI-1640 medium produced Standard *Leishmania major* promastigotes were washed three times in phosphate buffered saline. Then, RPMI-1640 medium was added to promastigotes and by means of hemocytometer, the concentration was adjusted to about 2.5×10^7 promastigotes/mL. To prepare the solution of compound I, RPMI-1640 medium was added to 20000 µg/mL concentration. The prepared solution was sterilized by filtration method. The dilution ratios of compound I in sterile 96 well microplates were

prepared between 10000 µg/mL and 312 µg/mL for antileishmanial activity test. Microdilution method with Alamarblue was applied as described in literature [28, 29]. After 24, 48 and 72 hours; visual evaluations were obtained, which are based on color changes. The effectiveness of compound I is indicated by the color change of Alamarblue in the wells. Turning of the color to pink indicates progress in parasite growth and no change in blue color indicates stopped growth of parasite, which can be interpreted, that compound I was effective. In order to observe the aliveness motions of promastigotes and to confirm it visually, 30 µL fresh samples were prepared from all wells and examined on microscope. The test was repeated twice for compound I and Amphotericin B was used as control medication.

Results and discussion*Geometry Optimizations*

The structure of the molecule, there is a phenyl ring and a benzothiophen moiety, which is consisted of 9 atoms. Due to the proton transfer between the oxygen atoms connected to C6 and C13 atoms, keto and enol tautomeric forms come to existence. The keto and enol tautomeric form of compound I, which has geometry optimization at DFT/B3LYP/6-311++G(d,p) level, is shown in Fig. 1 and some structural parameters are given Table 1. The total energies of keto and enol structures, corresponding their stable states were calculated as -755461.78 and -755444.54 kcal/mol respectively. The difference between total energies of keto and enol tautomeric forms is 17.24 kcal/mol. So much as the difference is keto tautomeric form more stable than enol tautomeric form. The dihedral angles between benzothiophen moiety and phenyl ring of keto and enol tautomeric structures of the molecule are 9.82 and 29.09°, respectively. Since the formation of tautomeric forms are based on proton transfer between oxygen atoms in the molecule, single bond lengths, double bond lengths and bond angles of these atoms were analyzed, where the atoms interact. In keto tautomeric form, the bond lengths C6–O11, C6–C1, C6=C5, C13=O15, C13–C14 and C13–C3 are 1.363, 1.396, 1.399, 1.226, 1.484 and 1.496 Å respectively, whereas the C6=O11, C6–C1, C6–C5, C13–O15 and C13–C14 bond lengths in enol tautomeric form are 1.232, 1.469, 1.469, 1.361, 1.441 Å respectively. These bond lengths were compared with bond lengths of similar structures in solid state and analyzed by X-ray diffraction in literature, the bond lengths of molecular structure in keto tautomeric form are 1.3447(10)/1.3573(16), 1.3945(13)/1.3908(17), 1.4144(12)/1.4083(16), 1.2359(11)/1.2297(15),

1.4954(13)/1.4926(17) and 1.4776(12)/1.4751(15) Å [30,31], respectively. Similarly, in literature given bond lengths for molecular structure in enol tautomeric form are 1.225(4)/1.237(3), 1.461(3)/1.501(3), 1.445(3)/1.501(3) Å [32], 1.406(3) and 1.515(3) Å [33], respectively. The bond angles of the molecule in keto and enol tautomeric forms are O11–C6–C1= 117.42/122.14, O11–C6–C5= 122.59/122.31, O15–C13–C14= 120.83/118.35 and O15–C13–C3= 120.11/116.79° respectively. The bond angles of single crystal molecules in literature, corresponding these bond angles are [117.45(8), 118.89(11)/120.9(3)], [122.56(8), 120.91(11)/121.2(2)], [120.17(8), 120.74(11)/111.46(17)], and [119.66(8), 119.50(11)/109.42(16)°] [30-33], respectively. It can be remarked, that the bond lengths and bond angles of O15 atom in enol tautomeric form differ a bit from data in literature. Similar molecules in literature have inter- and intramolecular hydrogen bonds. On the other hand, since the optimized structure is in gaseous state; there is not any such interactions and this is the reason of the difference. In both of two tautomeric forms, S32–C20 and S32–C16 bond lengths of

benzothiophen moiety are 1.748/1.750 and 1.769/1.770 Å, respectively. S32–C20–C22 bond angle in keto and enol tautomeric forms are 127.4/127.3°. The values in literature, that correspond these bond lengths and bond angles are 1.733(8)/1.7361(17), 1.757(9)/1.7496(16) Å and 125.7(7)/126.46(15)° [34, 35], respectively.

Since there is not any single crystal diffraction data of the molecule in both two tautomeric forms, their bond lengths and bond angles were compared with the bond lengths and bond angles of similar structures, which have X-ray diffraction data; in order to verify the chosen method and basis function for optimization of the structure. Generally, the structural parameters of optimized structure are accordant with structural parameters of similar structures in literature. The structural parameters in literature are data belonging to molecules in solid state. However, it must be considered, that the calculated molecular structure in tautomeric form is in gaseous phase.

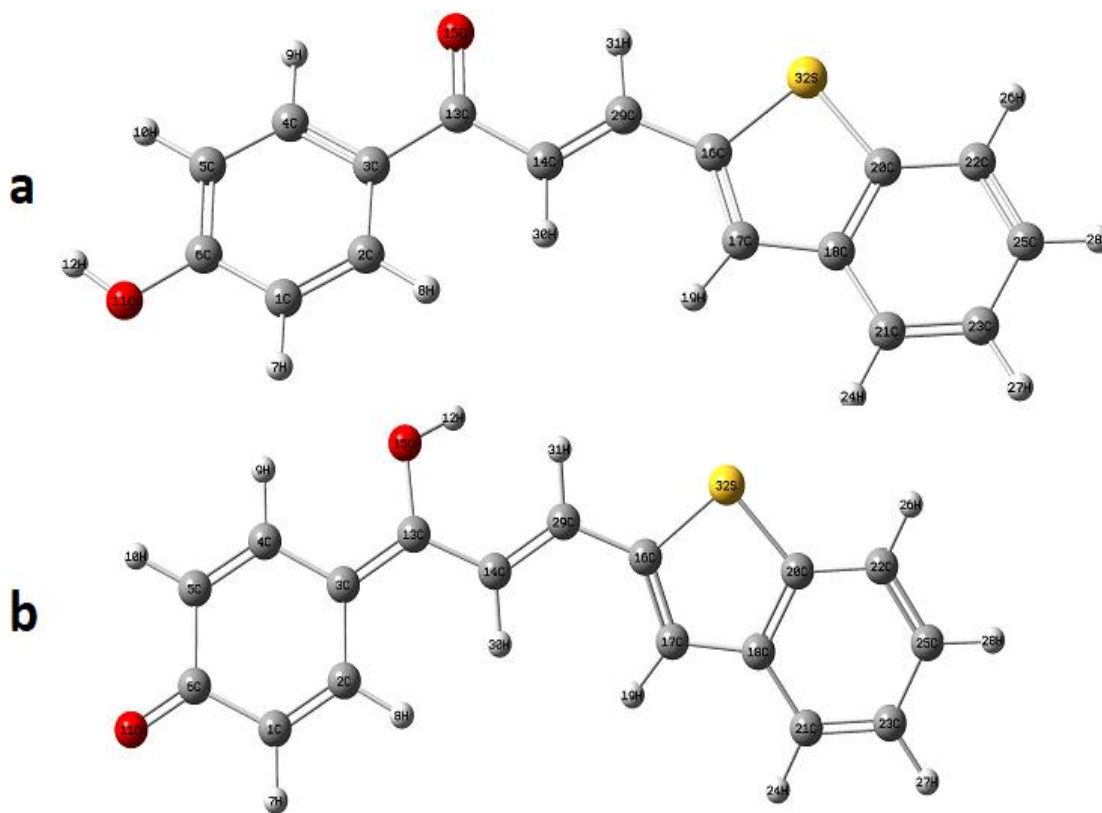


Fig. 1: The molecular structures of compound I obtained by DFT/B3LYP/6-311G(d,p) method for a) keto and b) enol form.

Table-1: Some structural parameters of compound I calculated by DFT/B3LYP/6-311++G(d,p) methods.

Bond Lengths (Å)	Keto		Enol		
	Keto	Enol	Keto	Enol	
C3-C4	1.403	1.447	C4-C3-C13	117.7	120.3
C4-C5	1.386	1.352	C2-C3-C13	124.3	122.5
C5-C6	1.399	1.469	O15-C13-C3	120.1	116.8
C6-O11	1.363	1.232	O15-C13-C14	120.8	118.4
C6-C1	1.396	1.469	C3-C13-C14	119.1	124.9
C1-C2	1.388	1.352	C14-C29-C16	126.4	125.5
C2-C3	1.404	1.447	C29-C16-S32	118.4	118.6
C3-C13	1.496	1.386	C29-C16-C17	130.2	130.0
C13-O15	1.226	1.361	S32-C20-C22	127.4	127.3
C13-C14	1.484	1.441	C17-C18-C20	112.1	112.2
C14-C29	1.348	1.357	C17-C18-C21	129.1	129.1
C29-C16	1.446	1.443	C21-C23-C25	120.8	120.8
C16-C17	1.370	1.372	C1-C2-C3	121.3	121.7
C17-C18	1.428	1.428	C3-C4-C5	121.3	121.7
C18-C20	1.418	1.418	TorsionAngles (°)		
S32-C20	1.748	1.750	O11-C6-C5-C4	179.9	-179.8
S32-C16	1.769	1.770	O11-C6-C1-C2	179.8	179.7
C20-C22	1.398	1.397	O15-C13-C3-C4	6.2	5.0
C22-C25	1.387	1.388	O15-C13-C3-C2	-173.0	-173.9
C23-C21	1.383	1.383	C16-C29-C14-C13	-179.3	-176.8
C21-C18	1.409	1.409	S32-C16-C29-C14	-178.7	-169.2
Bond angles (°)			S32-C20-C22-C25	-180.0	-179.9
O11-C6-C5	122.6	122.3	C29-C16-C17-C18	180.0	-179.7
O11-C6-C1	117.4	122.1	C17-C18-C21-C23	-180.0	179.9

Vibrational spectra and NMR spectra

The FTIR spectrum of compound I (Fig. 2) showed the characteristic bands of the -OH, C=O, aliphatic C=C and C-O groups at 3129, 1642, 1555 and 1275 cm⁻¹, respectively. These bands confirm predicted molecular structure of compound I.

The IR bands of keto and enol tautomeric forms of compound I were obtained in gase state by DFT/B3LYP/6-311++G(d,p) method. Some of calculated stretching bands (scaled) and experimental ones are presented in Table 2. IR vibrational band seen in Table 2 are agreement with those of experimental ones. But, especially O-H stretching band observed at 3129 cm⁻¹ as experimentally was calculated as 3668 and 3656 cm⁻¹ for keto and enol forms, respectively. The deviations calculated for O-H bands of keto and enol forms are 539 and 527 cm⁻¹, respectively and can be attributed O-H...O type strong intermolecular hydrogen bond. Intermolecular interaction suggested as O-H...O type strong intermolecular hydrogen bond in the molecular structure of compound I are shown in Fig. 3.

Table-2: Selected experimental and calculated vibrational frequencies (cm⁻¹).

Assignments*	Compound I				
	Calculated (Scaled)				
	Exp. IR (cm ⁻¹)	Keto		Enol	
Freq		I _{IR}	Freq.	I _{IR}	
v(O-H)	3129	3668	119.71	3656	49.92
v(C-H) _{arom.}	3026- 3100	3020- 3067	21.75- 5.59	3048- 3069	2.26- 12.67
v(C=O)	1642	1635	118.96	1652	699.21
v(HC=CH)	1555	1598	155.10	1598	119.27
v(C-O)	1275	1267	135.42	1353	107.24

NMR chemical shifts of keto and enol forms of compound I were calculated at DFT/B3LYP/6-

311++G (d,p) level by based on molecular structures optimized in DMSO solvent. ¹H- and ¹³C-NMR chemical shifts (scaled) of keto and enol tautomeric forms are given in Table-3 together with experimental ones. Spectrally observed chemical shifts for all protons and carbons are consistent with theoretical values, and in addition all results support that the structure of compound I is the keto form. ¹H- and ¹³C-NMR spectra of compound I are given in Fig. 4 and Fig. 5, respectively.

Table-3: ¹H isotropic chemical shifts (ppm) in DMSO for compound I.

Atom	Compound I		
	Experimental	Calculated (in DMSO)	
		Keto	Enol
C13	186.89	191.62	171.02
C6	162.88	170.01	193.78
C20	140.51	155.99	155.99
C16	139.94	152.49	151.89
C18	130.49	147.40	146.80
C29	136.46	142.84	137.50
C2	131.66	138.48	141.01
C4	131.66	137.89	139.99
C3	129.22	136.37	121.44
C25	123.49	133.12	133.60
C23	125.07	132.07	132.08
C21	126.95	131.54	132.65
C17	125.58	130.18	131.68
C22	140.09	128.91	129.06
C14	127.21	121.59	120.18
C5	115.99	121.07	133.26
C1	115.99	120.38	132.01
H9	8.04	8.5932	8.39
H8	8.04	8.5406	8.15
H19	7.96	8.3356	8.46
H30	7.58	8.2834	8.06
H24	8.44	8.2651	8.29
H26	7.90	8.1164	8.17
H31	7.98	8.0184	7.21
H28	8.01	7.78	7.74
H27	8.44	7.74	7.71
H7	6.92	7.32	6.58
H10	6.92	7.18	6.64
H12	10.52	5.22	6.20

Table-3 indicates that the O–H bands observed at 10.52 ppm are calculated as 5.22 ppm for keto form and 6.20 ppm for enol form. In NMR calculations, intermolecular interactions were not considered. For this reason, the deviations of 5.30 and 4.32 ppm for keto and enol forms, respectively in the OH signals can be associated with O–H···O type strong intermolecular hydrogen bond, as supported by the IR results.

As can be seen from the Fig. 3, the intermolecular hydrogen bond is formed between oxygen in the carbonyl group (C=O) of compound I and phenolic (OH) hydrogen. Compound I in this structure is in keto form. In the presence of the enol form, due to the deformation of the benzene ring, the molecular structure is unstable (molecular total energies; -755461.78 and -755444.54 kcal/mol for keto and enol form, respectively), and particularly NMR data well reflect the presence of the keto form.

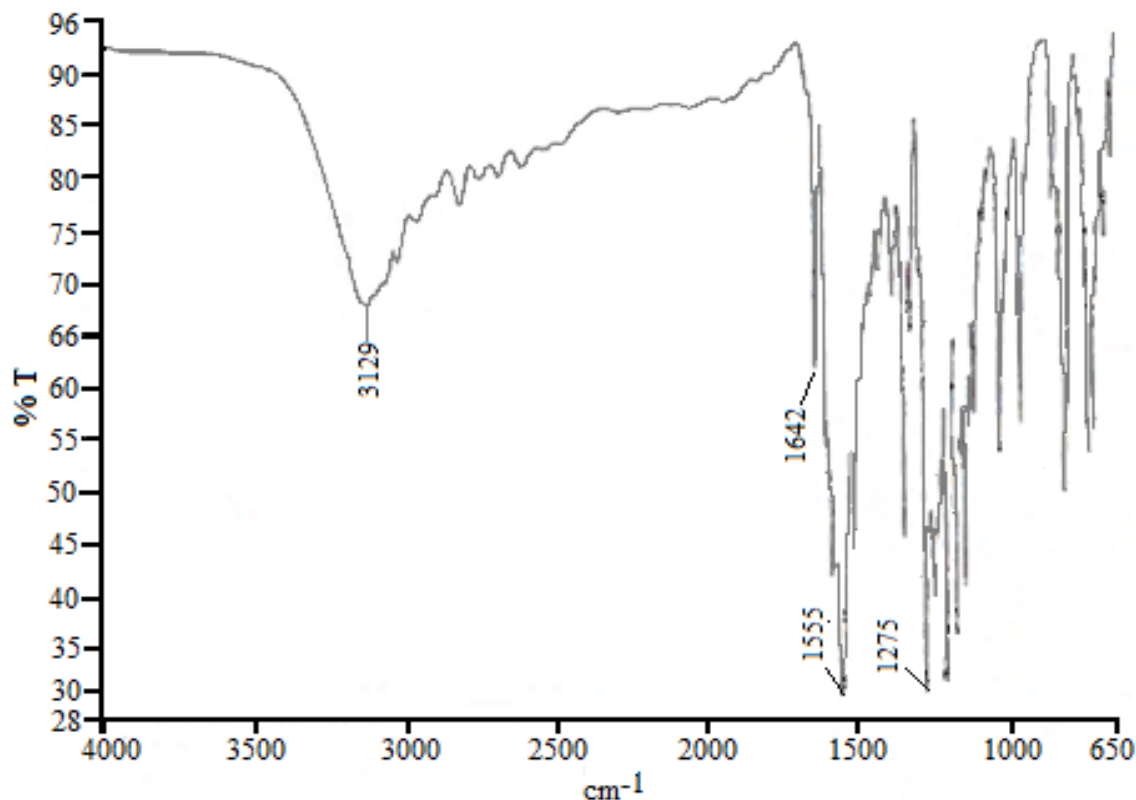


Fig. 2: FTIR spectrum of compound I.

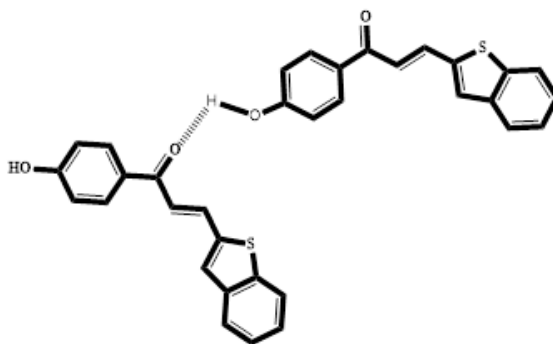
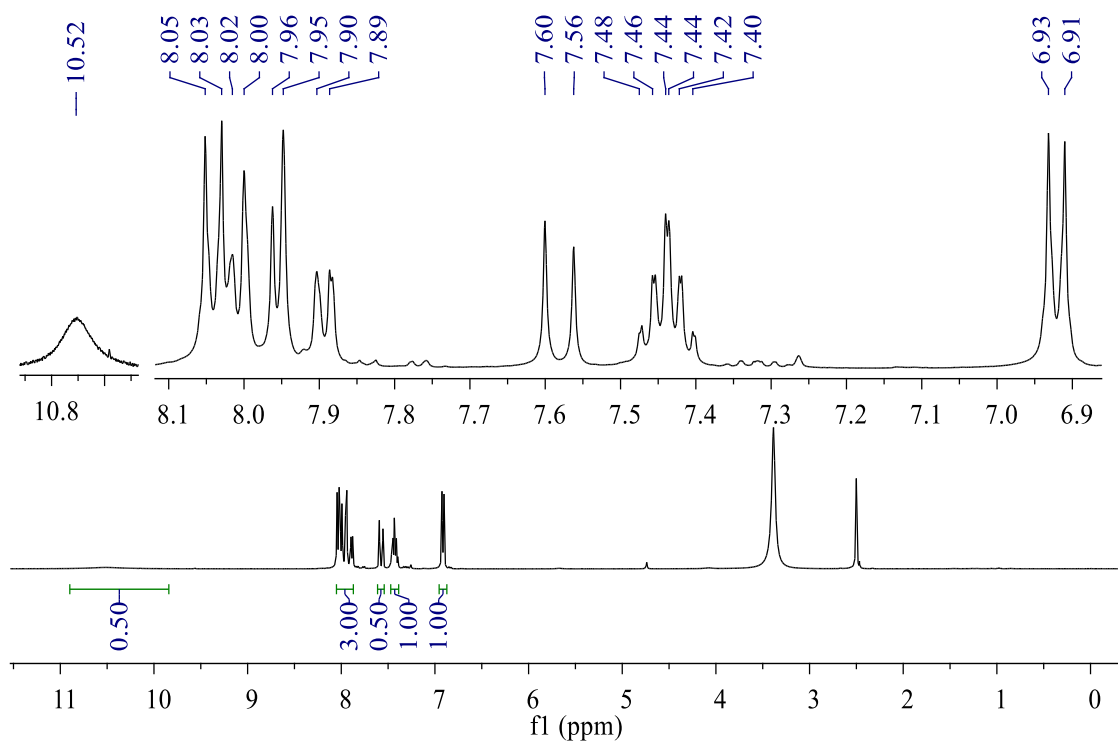
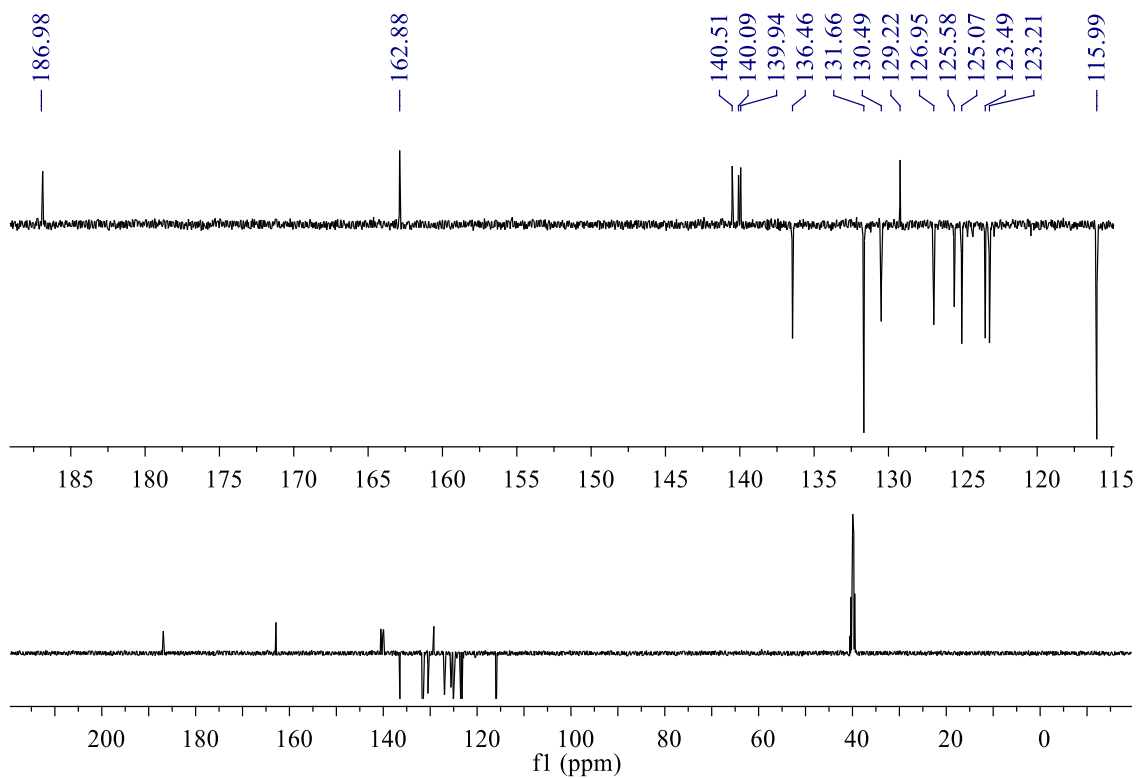


Fig. 3: The O–H···O type intermolecular strong hydrogen bond suggested between OH and O=C groups in the molecular structure of (2E)-3-(1-benzothiophen-2-yl)-1-(4-hydroxyphenyl)prop-2-en-1-one (I).

Fig. 4: ¹H-NMR spectra of compound I.Fig. 5: ¹³C-NMR spectra of compound I.

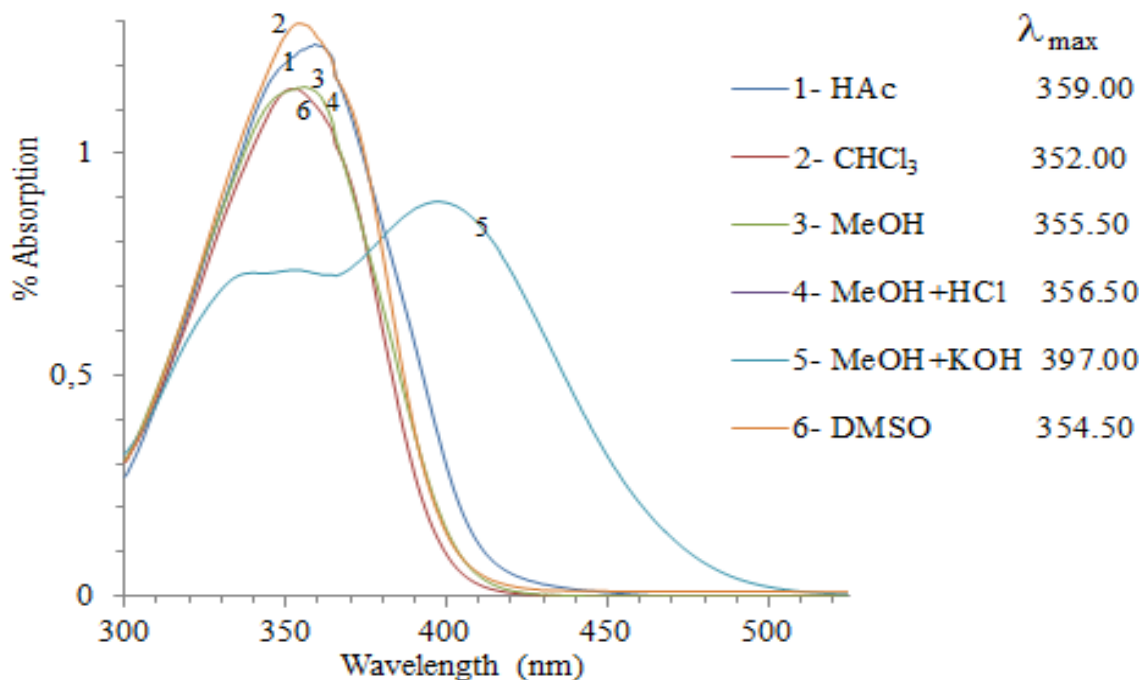


Fig. 6: UV-Vis spectra of compound I in studied solutions and obtained λ_{\max} values.

Absorption spectra

Methanol (MeOH), DMSO, HCl, KOH, Chloroform (CHCl₃) and acetic acid (HAc) used in the UV study were purchased from Merck. Stock solutions of compound I in MeOH, DMSO, HCl, KOH, CHCl₃ and HAc were prepared in the range of about 10⁻⁶-10⁻⁸ M. The UV-Vis spectra of the prepared stock solutions were recorded in the 300-800 nm range. The solution in methanol was divided into two parts. After spectra of compound I in methanol were taken; To the partitioned solution in MeOH was added 1 drop of 37% HCl and then the spectrum was taken. The 6 drops of methanolic solution prepared from 1.072 g of KOH and 100 mL of MeOH were added to the other partitioned solution of compound I in MeOH and the spectrum was taken. Recorded spectrums can be seen in Fig. 6 together with λ_{\max} .

As evaluated the UV-Vis absorption spectra of compound I given in Fig. 6, It is seen that compound I gives similar to each other spectra having a single λ_{\max} at average of 355.50 nm in the solvents used. For this reason, It can be said that in these solvents, compound I may exist in the keto tautomeric structure, which is probably the most stable of the possible tautomers shown in Fig. 1. From the ¹H- and ¹³C-NMR spectral data of compound I in DMSO (Figs. 4 and 5), it is confirmed that compound I has a single tautomeric structure and that the spectral data are compatible with the keto structure.

The solvents used can be arranged as CHCl₃ <HAc <MeOH <DMSO according to increasing dielectric constant. Dielectric constants of solvents are CHCl₃ (4.81), HAc (6.17), MeOH (32.66) and DMSO (44.45) [36]. λ_{\max} values of compound I in these solvents did not show a linear change as depending on the increase in dielectric constant. However, hypsochromic shift of 4.50 nm (5.90 nm theoretical bathochromic shift) in protic HAc and MeOH solvents, and a bathochromic shift of 2.50 nm (2.6 nm theoretical hypsochromic) was observed in non-protic CHCl₃ and DMSO solvents. In other words, compound I shows little bathochromic shift in protic solvents.

Phenol is known to be a weak organic acid. It is possible for compound I, a phenol derivative, to ionize in MeOH and DMSO solvents, which are proton acceptors. To determine this, when solutions of the concentrated HCl and KOH in methanol was added dropwise to separately MeOH stock solutions, and HCl was added, a bathochromic shift of 1 nm according to the λ_{\max} values of compound I in MeOH was observed, but, it did not cause any significant change in the spectrum. On the other hand, the addition of KOH was resulted as a hypsochromic shift of 3.00 nm according to the λ_{\max} values of compound I in MeOH and this led to the formation of a second absorption band with λ_{\max} values of 397.00 nm, unlike the spectrum in MeOH (Fig. 6). It can be said that compound I does not show ionization in the solvents used because the absorption bands in the solvents used are in the same location and in similar

shapes, the acid addition has no effect and the base addition results in a band having a second maximum in the bathochromic region. If there is ionization in the solvents used, it has that the absorption bands of compound I resembles the MeOH+KOH absorption band, or appear a shoulder on the bathochromic side [37]. As a result, according to all obtained spectral data, compound I is in a stable single form and has a partially ionizable structure in basic medium.

4-hydroxy-azobenzene in MeOH has an absorption band with three maximums of 235, 345 and 425 nm [38]. Among these values, only 425 nm is in the visible region. When the λ_{max} value at 345 nm of 4-hydroxy-azobenzene in methanol was compared with that of the compound I in MeOH, it shows a bathochromic shift of 10.50 nm and a hypsochromic shift of 69.50 nm relative to its value at 425 nm.

The compound I is yellow in the solid phase and forms colorless solutions in the solvents used. The yellow color is due to the intermolecular (OH \cdots O=C) hydrogen bonding interaction between the OH and O=C groups in compound I side [38]. The ionic structure of compound I in the basic medium produces a yellow absorption at 397 nm in the visible region, because it is similar to the structure of compound I in the solid phase having hydrogen bond interaction.

Theoretical absorption spectra of compound I in the solvents studied (MeOH, DMSO, CHCl₃ and HAc) were obtained at TD-DFT/B3LYP/6-311G++(d,p) level by using optimized structures of compound I in the same solvents. All calculations were performed for both keto and enol forms of compound I. The calculated absorption spectra of compound I have two absorption bands; for keto form, absorption wavelengths (λ) of bands in HAc, CHCl₃, MeOH and DMSO are 383.3/265.6 nm, 384.4/265.6 nm, 384.4/255.7 nm and 386.6/255.7 nm with oscillator strength being 0.637/0.101, 0.738/0.116, 0.632/0.151 and 0.644/0.152, respectively. For enol form, these λ values in studied solvents are 467.6/289.8 nm, 471.8/291.2 nm, 464.8/288.4 nm and 470.4/289.8 nm with oscillator strength being 1.389/0.196, 1.382/0.199, 1.366/0.191 and 1.389/0.198, respectively. Obtained λ values and those of experimental are given in Table 4.

The excitation energies corresponding to λ values of 383.3/265.6 nm, 384.4/265.6 nm, 384.4/255.7 nm and 386.6/255.7 nm obtained for keto form are 3.235/4.668 eV, 3.225/4.668 eV, 3.225/4.849 eV and 3.207/4.849 eV, respectively. Similarly, for enol form, excitation energies for absorption bands of 467.6/289.8 nm, 471.8/291.2 nm, 464.8/288.4 nm and 470.4/289.8 nm are 2.652/4.278 eV, 2.628/4.258 eV, 2.668/4.299 eV and 2.636/4.278 eV, respectively.

As can be seen from Table 4, in all solvent studied, calculated absorption bands are in the range of 383.3-386.6 nm and 464.8-471.8 nm for keto and enol forms, respectively. The theoretical λ values calculated for enol tautomeric form of compound I are 108.6-119.8 nm more than λ_{max} values observed in UV-Vis spectra of compound I, whereas those of values for keto tautomer are quite close (24.3-32.4 nm). In this case, it can be stated that UV data also confirm the presence of keto form for compound I. In addition, the experimentally observed bathochromic for non-protic solvents and hypsochromic shifts for protic are also obtained for theoretical results. The shifts are close to experimental values, but are opposite.

Table-4: Experimental and calculated absorption bands of compound I.

Solvent	Exp. λ_{max} (nm)	Calculated absorption wavelengths (λ) (nm)	
		Keto	Enol
HAc	359.0	383.3/265.6	467.6/289.8
CHCl ₃	352.0	384.4/265.6	471.8/291.2
MeOH	355.5	384.4/255.7	464.8/288.4
DMSO	354.5	386.6/255.7	470.4/289.8

Frontier molecular orbitals (FMOs) in studied solvents of keto and enol forms of compound I were calculated by using DFT/B3LYP/6-311++G(d,p) method. For both keto and enol forms of compound I in the each of solvents, E_{HOMO} , E_{LUMO} energies and $\Delta E_{\text{HOMO-LUMO}}$ energy differences were obtained and, these values were used to calculate the quantum chemical parameters; taking into account that $I = -E_{\text{HOMO}}$ and $A = -E_{\text{LUMO}}$, using the definitions in the literature [39,40], hardness (η) chemical potential (μ), electronegativity (χ) and electrophilicity (ω). Results are presented in Table 5. Frontier molecular orbitals (as HOMO and LUMO) for keto and enol form together with energy values can be seen Fig. 7.

UV absorption spectra data of compound I were detailed by investigating the probable transitions between electronic energy levels of keto and enol forms of compound I in solvent studied. The results show that between HOMOs and LUMOs, ten possible electronic transitions are defined, and for each studied state, the most possible transitions are as HOMO-1 \rightarrow LUMO and HOMO \rightarrow LUMO transitions for keto and enol forms, respectively. Absorption wavelengths (in nm) (with oscillator strengths) corresponding these electronic transitions for keto and enol forms, respectively are 362.1 nm (0.493)/473.1 nm (1.357), 362.1 nm (0.482)/476.6 nm (1.405), 363.5 nm (0.500)/471.9 nm (1.284) and 364.4 (0.481)/476.5 nm (1.331) for HAc, CHCl₃, MeOH and DMSO, respectively. It is concluded that the most possible transitions in the range of 362.10-364.40 for keto are very consistent with experimental ones and confirm presence of keto form for compound I.

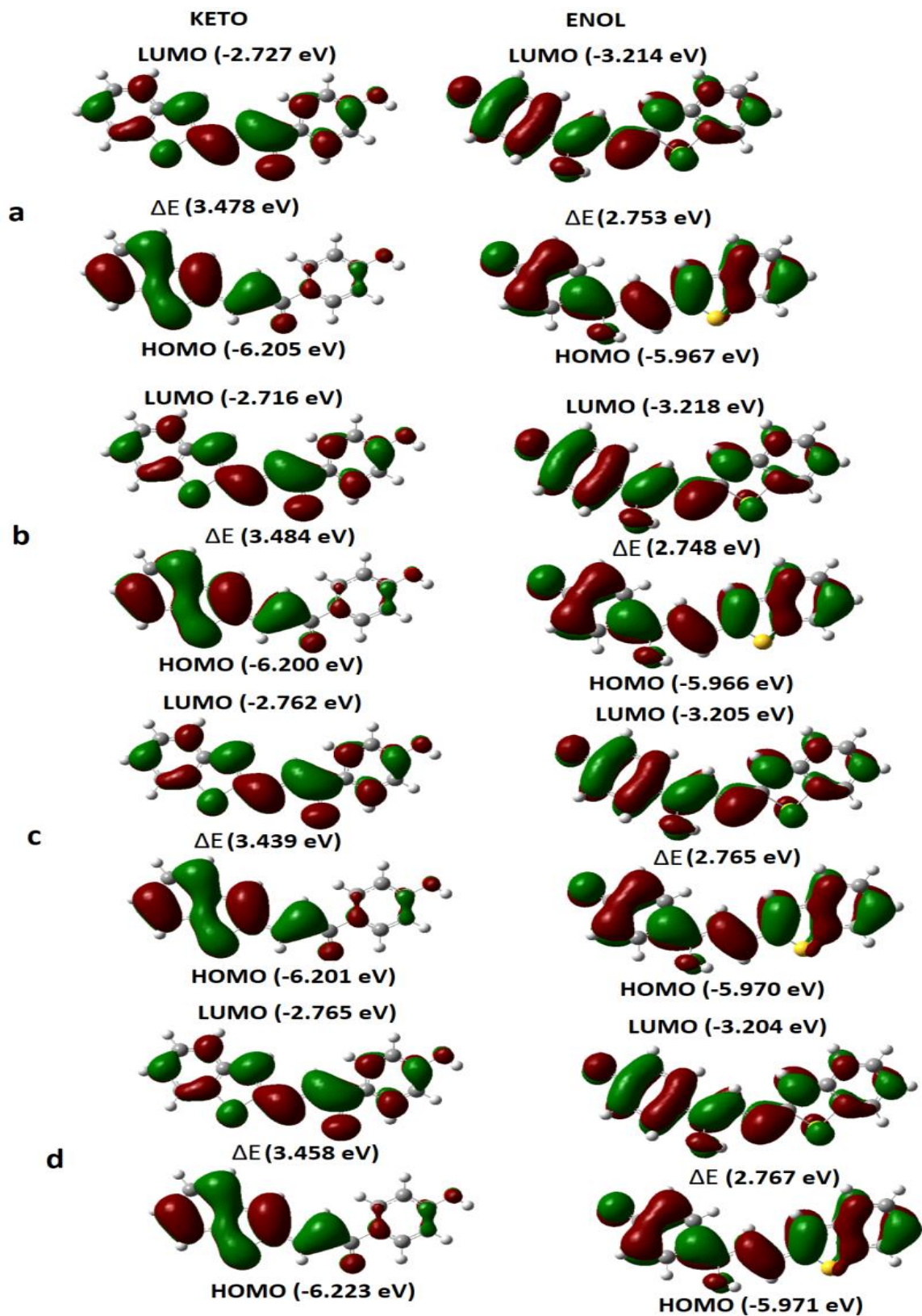


Fig. 7: Molecular orbital surfaces and energy levels (given in parentheses) for the HOMO and LUMO of keto and enol forms of compound I in a) HAc , b) CHCl₃, c) MeOH, d) DMSO

Table-5: Calculated energy values (in eV) in different solvents of two tautomeric forms of the compound I by B3LYP/6-311++G (d,p) method

	Keto				Enol			
	HAc	CHCl ₃	MeOH	DMSO	HAc	CHCl ₃	MeOH	DMSO
HOMO (eV)	-6.205	-6.200	-6.201	-6.223	-5.967	-5.966	-5.970	-5.971
LUMO (eV)	-2.727	-2.716	-2.762	-2.765	-3.214	-3.218	-3.205	-3.204
Energy gap (eV)	3.478	3.484	3.439	3.458	2.753	2.748	2.765	2.767
Ionization potential, I (eV)	6.205	6.200	6.201	6.223	5.967	5.966	5.970	5.971
Electron affinity, A (eV)	2.727	2.716	2.762	2.765	3.214	3.218	3.205	3.204
Chemical potential, μ (eV)	-4.466	-4.458	-4.482	-4.494	-4.591	-4.592	-4.588	-4.588
Electronegativity, χ (eV)	4.466	4.458	4.482	4.494	4.591	4.592	4.588	4.588
Chemical hardness, η (eV)	1.739	1.742	1.720	1.729	1.377	1.374	1.383	1.384
Chemical softness, σ (eV) -1	0.575	0.574	0.581	0.578	0.726	0.728	0.723	0.723
Electrophilicity, ω (eV)	5.734	5.704	5.839	5.840	7.653	7.673	7.610	7.605

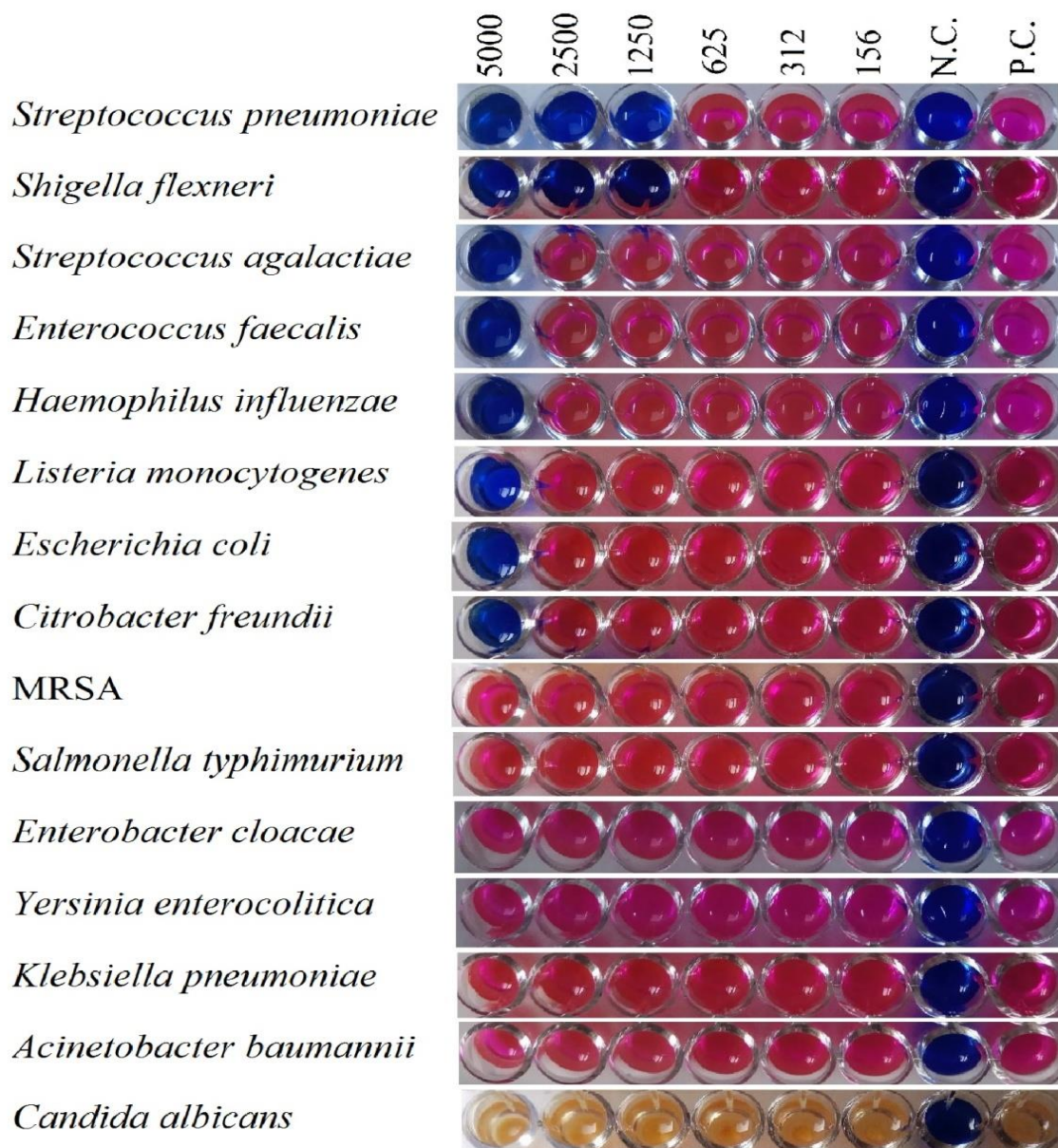
Fig. 8: Antibacterial and antifungal activities results of compound I. Dilution concentrations; 5000-156 $\mu\text{g/mL}$. N.C.: Negative Control; P.C.: Positive Control.



Fig. 9: Antileishmanial activity results of compound I against standard *Leishmania major* promastigotes. Control drug: Amphotericin B. Dilution concentrations 10000-312 µg/mL. N.C.: Negative Control; P.C.: Positive Control.

The results of in vitro antimicrobial activity

The antibacterial activities of compound I against bacterial isolates tested are shown in Fig. 8. MIC values determined for compound I are given in Table 6.

Compound I have different levels of antibacterial activity against to eight standard bacteria (*Streptococcus pneumoniae*, *Shigella flexneri*, *Streptococcus agalactiae*, *Enterococcus faecalis*, *Haemophilus influenzae*, *Listeria monocytogenes*, *Escherichia coli* and *Citrobacter freundii* isolates). MIC values were obtained as 1250-5000 µg/mL. No antimicrobial activity was detected at the concentrations studied against other six bacteria and one fungi in the study.

Antileishmanial activity test result of compound I was given in Fig. 9. Compound I have antileishmanial activity (MIC: 5000 µg/mL) against *Leishmania major* promastigotes. Amphotericin B used as standard drug was effective at all concentrations (MIC: <312 µg/mL) for *Leishmania major* promastigotes.

Table-6: Minimum inhibitory concentration (MIC) values of compound I against microorganisms studied.

Standard isolates	MIC values (µg/ml)
<i>Acinetobacter baumannii</i>	>5000
<i>Salmonella typhimurium</i>	>5000
MRSA	>5000
<i>Klebsiella pneumoniae</i>	>5000
<i>Enterobacter cloacae</i>	>5000
<i>Yersinia enterocolitica</i>	>5000
<i>Candida albicans</i> *	>5000
<i>Leishmania major</i> **	5000
<i>Streptococcus agalactiae</i>	5000
<i>Citrobacter freundii</i>	5000
<i>Escherichia coli</i>	5000
<i>Enterococcus faecalis</i>	5000
<i>Haemophilus influenzae</i>	5000
<i>Listeria monocytogenes</i>	5000
<i>Streptococcus pneumoniae</i>	1250
<i>Shigella flexneri</i>	1250

*fungi, **parasite

Conclusions

In this study, (2E)-3-(1-benzothiophen-2-yl)-1-(4-hydroxyphenyl)prop-2-en-1-one (I) was synthesized and characterized by IR, NMR and LC-MS/MS methods. The theoretical study was performed for two probable tautomeric form as keto and enol by DFT/B3LYP/6-311++G(d,p) method. IR, NMR and UV spectral data of keto and enol form of compound I were calculated and compared with those of experimental ones. The deviations obtained in the between experimental and theoretical spectral data of IR and NMR point out O-H...O type strong intermolecular hydrogen bond. Other spectral data are consistent with theoretical values that support compound I is in the keto form. UV-Vis spectra of compound I in CHCl₃, HAc, MeOH and DMSO solvents were compared with absorption spectra calculated using TD-DFT/B3LYP/6-311++G(d,p) method. Results confirm that compound I is in keto form. The antibacterial, antifungal and antiparasitic activities of compound I were evaluated by using MIC values determined by microdilution broth method with Alamarblue. Tests were performed against fourteen different bacteria, one fungi and one *Leishmania* species. According to the test results; compound I is effective on eight different bacterial species (MIC: 1250-5000 µg/mL) and has the antileishmanial activity (MIC: 5000 µg/mL). Therefore, further studies can be planned on this compound. To use the synthesized compound as a drug candidate, control studies, the toxicity tests on the experimental animal models of compound I are required.

Acknowledgement

The numerical calculations reported in this paper were fully performed at TUBITAK ULAKBIM, High Performance and Grid Computing Center (TRUBA resources).

References

1. E. Polo, N. Ibarra-Arellano, L. Prent-Peñalosa, A. Morales-Bayuelo, J. Henao, A. Galdámez, M. Gutiérrez, Ultrasound-assisted synthesis of novel chalcone, heterochalcone and bis-chalcone derivatives and the evaluation of their antioxidant properties and as acetylcholinesterase inhibitors, *Bioorg. Chem.*, **90**, 103034 (2019).
2. N. Yaylı, M. Küçük, O. Üçüncü, A. Yaşar, N. Yaylı, Ş. A. Karaoğlu, Synthesis of N-alkyl derivatives and photochemistry of nitro (E)-3-azachalcones with theoretical calculations and biological activities, *J. Photoch. Photobiology A: Chemistry*, **188**, 161 (2007).
3. A. Usta, A. Yaşar, N. Yılmaz, C. Güleç, N. Yaylı, Ş. A. Karaoğlu, N. Yaylı, Synthesis, Configuration, and Antimicrobial Properties of Novel Substituted and Cyclized '2,3"-Thiazachalcones, *Helv. Chim. Acta.*, **90**, 1482 (2007)
4. N. Kahriman, N. Y. İskender, M. Yücel, N. Yaylı, E. Demir, Z. Demirbağ, Microwave-assisted synthesis of 1, 3'-diaza-flavanone/flavone and their alkyl derivatives with antimicrobial activity, *J. Heterocyclic Chem.*, **49**, 71 (2012)
5. A. Nas, N. Kahriman, H. Kantekin, N. Yaylı, M. Durmuş, The synthesis of novel unmetallated and metallated phthalocyanines including (E)-4-(3-cinnamoylphenoxy) groups at the peripheral positions and photophysicochemical properties of their zinc phthalocyanine derivatives, *Dyes and Pigments.*, **99**, 90 (2013)
6. N. Kahriman, V. Serdaroğlu, K. Peker, A. Aydın, A. Usta, S. Fandaklı, N. Yaylı, Synthesis and biological evaluation of new 2, 4, 6-trisubstituted pyrimidines and their N-alkyl derivatives, *Bioorg. Chem.*, **83**, 580 (2019).
7. H. Zaki, A. Belhassan, A. Aouidate, T. Lakhli, M. Benlyas, M. Bouachrine, Antibacterial study of 3-(2-amino-6-phenylpyrimidin-4-yl)-N-cyclopropyl-1-methyl-1H-indole-2-carboxamide derivatives: CoMFA, CoMSIA analyses, molecular docking and ADMET properties prediction, *J. Mol. Struct.*, **1177**, 275 (2019).
8. A. Singh, P. K. Gautam, A. Verma, V. Singh, P. S. Priya, S. Shivalkar, S. K. Samanta, Green synthesis of metallic nanoparticles as effective alternatives to treat antibiotics resistant bacterial infections: A review, *Biotechnology Reports*, **25**, e00427 (2020)
9. E. A. A. Elsalam, H. F. Shabaiek, M. M. Abdelaziz, I. A. Khalil, I. M. El-Sherbiny, Fortified hyperbranched PEGylated chitosan-based nano-in-micro composites for treatment of multiple bacterial infections, *Int. J. Biol. Macromol.*, **148**, 1201 (2019).
10. E. Torres-Guerrero, M. R. Quintanilla-Cedillo, J. Ruiz-Esmenjaud, R. Arenas, Leishmaniasis: a review, *F1000Research*, **6**, 1 (2017).
11. G. A. N. Pereira, E. B. Silva, S. F. P. Braga, P. G. Leite, L. C. Martins, R. P. Vieira, W. T. Soh, F. S. Villela, F. M. R. Costa, D. Ray, S. F. Andrade, H. Brandstetter, R. B. Oliveira, C. R. Caffrey, F. S. Machado, R. S. Ferreira, Discovery and characterization of trypanocidal cysteine protease inhibitors from the 'malaria box', *Eur. J. Med. Chem.*, **179**, 765 (2019).
12. M. Den Boer, D. Argaw, J. Jannin, J. Alvar, Leishmaniasis impact and treatment access, *Clin. Microbiol. Infect.*, **17**, 1471 (2011).
13. A. Sabur, M. Asad, N. Ali, Lipid based delivery and immuno-stimulatory systems: Master tools to combat leishmaniasis, *Cell Immunol.*, **309**, 55 (2016).
14. M. J. Frisch, G. W. Trucks, H. B. Schlegel, G. E. Scuseria, M. A. Robb, J. R. Cheeseman, G. Scalmani, V. Barone, B. Mennucci, G. A. Petersson, H. Nakatsuji, M. Caricato, X. Li, H. P. Hratchian, A. F. Izmaylov, J. Bloino, G. Zheng, J. L. Sonnenberg, M. Hada, M. Ehara, K. Toyota, R. Fukuda, J. Hasegawa, M. Ishida, T. Nakajima, Y. Honda, O. Kitao, H. Nakai, T. Vreven, J. A. Montgomery Jr, J. E. Peralta, F. Ogliaro, M. Bearpark, J. J. Heyd, E. Brothers, K. N. Kudin, V. N. Staroverov, R. Kobayashi, J. Normand, K. Raghavachari, A. Rendell, J. C. Burant, S. S. Iyengar, J. Tomasi, M. Cossi, N. Rega, J. M. Millam, M. Klene, J. E. Knox, J. B. Cross, V. Bakken, C. Adamo, J. Jaramillo, R. Gomperts, R. E. Stratmann, O. Yazyev, A. J. Austin, R. Cammi, C. Pomelli, J. W. Ochterski, R. L. Martin, K. Morokuma, V. G. Zakrzewski, G. A. Voth, P. Salvador, J. J. Dannenberg, S. Dapprich, A. D. Daniels, O. Farkas, J. B. Foresman, J. V. Ortiz, J. Cioslowski, D. J. Fox, Gaussian 09 Revision A.1, Gaussian Inc., Wallingford, CT, (2009).
15. R. D. Dennington, T. A. Keith, J. M. Millam, Gauss View, Version 5.0, Semichem Inc., Shawnee Mission, KS (2009).
16. A. D. Becke, Perspective on "Density functional thermochemistry. III. The role of exact exchange, *J. Chem. Phys.*, **98**, 5648 (1993).
17. C. Lee, W. Yang, R. G. Parr, Development of the Colle-Salvetti correlation-energy formula into a functional of the electron density, *Phys. Rev. B*, **37**, 785 (1998).
18. A. Abbas, H. Gökçe, S. Bahçeli, M. M. Naseer, Spectroscopic (FT-IR, Raman, NMR and UV-vis.) and quantum chemical investigations of (E)-

- 3-[4-(pentyloxy)phenyl]-1-phenylprop-2-en-1-one, *J. Mol. Struct.*, **1075**, 352 (2014).
- H. Gökçe, N. Öztürk, M. Taşan, Y. B. Alpaslan, G. Alpaslan, Spectroscopic characterization and quantum chemical computations of the 5-(4-pyridyl)-1H-1,2,4-triazole-3-thiol molecule, *Spectrosc. Lett.*, **49**, 167 (2016).
 - R. Ditchfield, Molecular Orbital Theory of Magnetic Shielding and Magnetic Susceptibility, *J. Chem. Phys.*, **56**, 5688 (1972).
 - K. Wolinski, J. F. Hinton, P. Pulay, Efficient implementation of the gauge-independent atomic orbital method for NMR chemical shift calculations, *J. Am. Chem. Soc.*, **112**, 8251 (1990).
 - Y. B. Alpaslan, H. Gökçe, G. Alpaslan, M. Macit, Spectroscopic characterization and density functional studies of (Z)-1-[(2-methoxy-5-(trifluoromethyl) phenylamino) methylene] naphthalene-2(1H)-one, *J. Mol. Struct.*, **1097**, 171 (2015).
 - Y. B. Alpaslan, N. Süleymanoğlu, R. Ustabaş, A. G. Ertürk, H. Gökçe, Spectroscopic characterization and density functional studies of new thiadiazole 1,1-dioxide compounds, *J. Mol. Struct.*, **1174**, 32 (2018).
 - R. E. Stratmann, G. E. Scuseria, M. J. Frisch, An efficient implementation of time-dependent density-functional theory for the calculation of excitation energies of large molecules, *J. Chem. Phys.*, **109**, 8218 (1998).
 - R. Bauernschmitt, R. Ahlrichs, Treatment of electronic excitations within the adiabatic approximation of time dependent density functional theory, *Chem. Phys. Lett.*, **256**, 454 (1996).
 - M. S. Engin, S. Demir, Ş. Direkel, S. Eymur, S. Çay, A. Güder, Synthesis, characterization, biological activity, and DFT-reactivity assessment of Mn(II), Co(II), and Cu(II) complexes of a new N₂O tridentate Schiff base, *Russ. J. Gen. Chem.*, **86**, 2855 (2016).
 - N. O. İskeleli, Y. B. Alpaslan, Ş. Direkel, A. G. Ertürk, N. Süleymanoğlu, R. Ustabaş, The new Schiff base 4-[(4-Hydroxy-3-fluoro-5-methoxybenzylidene)amino]-1,5-dimethyl-2-phenyl-1,2-dihydro-pyrazol-3-one: Experimental, DFT calculational studies and in vitro antimicrobial activity, *Spectrochim. Acta A*, **139**, 356 (2015).
 - M. Er, A. Ozer, Ş. Direkel, T. Karakurt, H. Tahtacı, Novel substituted benzothiazole and Imidazo[2,1-b][1,3,4]Thiadiazole derivatives: Synthesis, characterization, molecular docking study, and investigation of their in vitro antileishmanial and antibacterial activities, *J. Mol. Struct.*, **1194**, 284 (2019).
 - N. Süleymanoğlu, R. Ustabaş, Ş. Direkel, Y. B. Alpaslan, Y. Ünver, 1,2,4-triazole derivative with Schiff base; thiol-thione tautomerism, DFT study and antileishmanial activity, *J. Mol. Struct.*, **1150**, 82 (2017).
 - J. Hübscher, R. Rosin, W. Seichter, E. Weber, Crystal structures of 2-acetyl-4-ethynylphenol and 2-acetyl-4-(3-hydroxy-3-methylbut-1-yn-1-yl)phenol, *Acta Crystallogr. Sect. E*, **72**, 1370 (2016).
 - J. Hübscher, L. Izotova, S. Talipov, F. Eissmann, E. Weber, 1-(5-Acetyl-2-hydroxyphenyl)ethanone, *Acta Crystallogr. Sect. E*, **67**, o1622 (2011).
 - M. Akkurt, J. P. Jasinski, S. K. Mohamed, O. A. A. Allah, A. H. Tamam, M.R. Albayati, Crystal structure of 3-(9H-carbazol-9-yl)-N'-[(E)-4-chlorobenzylidene]propanohydrazide, *Acta Crystallogr. Sect. E*, **71**, o963 (2015).
 - R. S. Sancheti, A. G. Dikundwar, R. S. Bendre, 2-[[[2-Hydroxy-3-[2-methyl-5-(propan-2-yl)phenoxy]propyl](pyridin-2-ylmethyl)amino]methyl]phenol, *Acta Crystallogr. Sect. E*, **67**, o1605 (2011).
 - M. Parvez, S. T. E. Mesher, P. D. Clark, 2,3,6,7-Tetrakis(methylthio)benzo[b]thiophene, *Acta Crystallogr. Sect. C*, **52**, 1248 (1996).
 - P. Sugumar, S. Ranjith, J. A. Clement, A. K. Mohanakrishnan, M. N. Ponnuswamy, 5,7-Bis(1-benzothiophen-2-yl)-2,3-dihydrothieno[3,4-b][1,4]dioxine, *Acta Crystallogr. Sect. E*, **64**, o1049-o1049 (2008).
 - C. Reichardt, Wiley New York (1990).
 - N. A. Ateş, H. Berber, M. Yaman, Synthesis, Characterization And Spectroscopic Studies On Tautomerism And Acidity Constants Of Certain 4-(Phenyldiazenyl) Benzene-1,3-Diol Derivatives, *Anadolu Univ. J. Sci. And Tech. B-Theo. Sci.*, **4**, 11 (2016).
 - L. A. Kazitsyna, N. B. Kupletskaya, V. A. Ptsitsyna, O. A. Reutov, Some peculiarities of para-hydroxyazobenzene, *Div. Chem. Sci.*, **15**, 1414 (1966).
 - R. G. Pearson, Absolute electronegativity and hardness: applications to organic chemistry, *J. Org. Chem.*, **54**, 1423 (1989).
 - P. K. Chattaraj, U. Sarkar, D. R. Roy, Electrophilicity Index, *Chem. Rev.*, **106**, 2065 (2006).